# Paleovegetation seesaw in Brazil since the Late Pleistocene: A multiproxy study of two biomes

Vitor Azevedo [a,b,*], Nicolás M. Strikis [a], Valdir F. Novello [b], Camila L. Roland [a], Francisco W. Cruz [b], Roberto V. Santos [c], Mathias Vuille [d], Giselle Utida [b], Fábio Ramos Dias De Andrade [b], Hai Cheng [e,f], R. Lawrence Edwards [f]

[a] *Departamento de Geoquímica, Universidade Federal Fluminense, 24020-141 Niterói, Brazil*
[b] *Instituto de Geociências, Universidade de São Paulo, 05508-080 São Paulo, Brazil*
[c] *Instituto de Geociências, Universidade de Brasília, 70910-900 Brasília, Brazil*
[d] *Department of Atmospheric and Environmental Sciences, University at Albany, Albany, NY, USA*
[e] *Institute of Global Environmental Change, Xi'an Jiaotong University, 710049 Shaanxi, China*
[f] *Department of Earth Sciences, University of Minnesota, Minneapolis, MN 55455, USA*

## ARTICLE INFO

## ABSTRACT

Paleovegetation studies in Brazil have been mostly based on pollen analysis and geochemical proxies in lacustrine and soil records. These records, however, are sparsely located in the continent and, in most of the cases, centered over the Holocene, giving a minor picture of past vegetation since the Last Glacial Maximum. Stalagmites have been long used as recorders of paleoprecipitation and monsoon activity over time in tropical and subtropical South America by using $\delta^{18}O$ analyses, but recently they also showed the potential to record past vegetation and soil changes through the combined use of $\delta^{13}C$ and $^{87}Sr/^{86}Sr$. We utilize this new approach to determine the periods of paleovegetation transition and soil development in the Cerrado (Brazilian savanna) biome from central Brazil. Our results show a coherent period of transition from sparser vegetation and shallower soil above the cave to denser vegetation and thicker soil since the last deglaciation circa 15 ka BP. The timing of this transition is different from the multiproxy evidence found in the Caatinga (dry forest) biome, in northeastern Brazil, circa 4.2 ka BP, resulting in a period of paleovegetation seesaw pattern between central and northeastern regions of Brazil. Additionally, atmospheric $pCO_2$ and temperature variations may have played a major role on the paleovegetation transition in the Cerrado region whereas precipitation linked to the Intertropical Convergence Zone was the major modulator of paleovegetation in the Caatinga.

© 2021 Elsevier B.V. All rights reserved.

## 1. Introduction

Paleovegetation studies in Brazil are predominantly carried out on soil and lacustrine records, which document changes in paleotemperature, paleoprecipitation and paleovegetation through the use of pollen and other organic and inorganic proxies. Some of these records, however, are subjected to weathering processes and rarely exhibit deep, suitable horizons for radiometric dating to estimate change in sedimentation rates. Thus, these limitations complicate their use for reconstructing chronologically robust age-models, necessary to understand rapid paleoenvironmental changes over long time periods. Additionally, the scarcity of

lake records embracing the whole Last Glacial Maximum (LGM)-Holocene transition over the central South American region prevents us to understand how tropical biomes respond to changes in temperature, atmospheric $CO_2$, and rainfall. Therefore, alternative proxy records are needed to fill up existing gaps in paleoenvironmental reconstructions and better constrain abrupt environmental changes during Glacial-Interglacial cycles.

The $\delta^{18}O$ values in stalagmites from South America have long been used to reconstruct the South American Monsoon System (SAMS) activity (Wang et al., 2004, 2007; Cruz et al., 2005, 2009; Stríkis et al., 2011, 2015, 2018; Cheng et al., 2013a; Novello et al., 2016, 2017, 2018; Azevedo et al., 2019) with precise geochronology provided by the U-Th dating method (Cheng et al., 2000, 2013b; Shen et al., 2012). Additionally, recent studies based on the combination of $\delta^{13}C$ and $^{87}Sr/^{86}Sr$ analyses in stalagmites from Brazil have shown promising results, reconstructing past soil and

vegetation dynamics (Novello et al., 2019; Ward et al., 2019; Utida et al., 2020).

The $\delta^{13}C$ and $^{87}Sr/^{86}Sr$ values measured in stalagmites from Jaraguá cave (JAR record), located in the Cerrado (Brazilian savanna) portion of central-western Brazil (Novello et al., 2019), indicate the presence of shallow soil and sparse vegetation above the cave during the Late Pleistocene, followed by the development of thicker soil and denser vegetation during the deglaciation and Holocene. The paleovegetation documented in these stalagmites is coherent with other proxies measured in a sedimentary profile within the same cave (Novello et al., 2019) and the onset of warmer conditions and development of the current Cerrado vegetation (Whitney et al., 2011; Fornace et al., 2016), suggesting a transition for the region of the JAR record at circa 11.7 ka BP (Novello et al., 2019). The $\delta^{18}O$ record from the same stalagmites, however, shows that the SAMS was weaker during the Holocene and stronger during the LGM (Novello et al., 2017), indicating that the paleovegetation response to the SAMS activity was limited or absent.

A similar study, carried out in caves located in the Caatinga (dry forest) portion of the Northeast Brazil region (Utida et al., 2020), shows a different scenario, with denser vegetation and thicker soil from the Late Pleistocene to the Mid-Holocene, transitioning at circa 4.2 ka BP to an environment characterized by sparser vegetation and shallower soil development over the Late Holocene. In this region, however, the period with denser vegetation and thicker soil development coincides with wetter conditions and vice versa. Additionally, a paleoprecipitation dipole was previously described between the mid-western (SAMS core-region) and the northeastern regions of South America: with stronger activity in the former and weaker conditions in the later during the LGM, followed by a reverse scenario during the Holocene (Cruz et al., 2009; Cheng et al., 2013a).

Considering the problems of lacustrine records and the different paleoenvironment conditions described above, we combine $\delta^{13}C$ and $^{87}Sr/^{86}Sr$ from a suite of speleothems from Lapa Sem Fim (LSF) and Lapa Grande (LG) caves, located in central-eastern Brazil, to gain a better insight into the paleoenvironment, soil and vegetation changes and its relations to temperature, atmospheric $CO_2$, local hydrology and the paleoprecipitation dipole since the LGM. The study site embraces an important ecotonal zone, near the border between the Cerrado and Caatinga biomes.

## 2. Materials and methods

### 2.1. Study site

The stalagmite samples were collected in Lapa Sem Fim (LSF - 16°09′S, 44°36′W) and Lapa Grande (LG - 14°22′S, 44°17′W) caves (Fig. 1). These sites are within the NW-SE oriented convective band called the South Atlantic Convergence Zone (SACZ), one of the main components of the SAMS, with local average annual precipitation of 930 mm (period 1975-2009) based on meteorological stations (ANA-National Water Agency database). The bulk of precipitation at both sites occurs during the mature phase of the SAMS, between November-February (Stríkis et al., 2015). The karst system is placed within the Sete Lagoas (LG) and Lagoa do Jacaré (LSF) formations, carbonate units from the Bambuí Group, which is formed by siliciclastic and biochemical marine sediments deposited at circa 790-600 Ma ago (Santos et al., 2000). The local vegetation is predominant semi-deciduous forest typical of the border between Cerrado and Caatinga (Figure S6).

### 2.2. Samples

Five stalagmites from Lapa Sem Fim Cave (LSF3, LSF15, LSF16, LSF17 and LSF19), hereafter the LSF record, were analyzed for $\delta^{18}O$, $\delta^{13}C$ and $^{87}Sr/^{86}Sr$ and two stalagmites from Lapa Grande Cave (LG3 and LG11), hereafter the LG record, for $\delta^{18}O$ and $\delta^{13}C$. The $\delta^{18}O$ values from stalagmites LSF3, LSF15, LSF16, LG3 and LG11 were previously published by Stríkis et al. (2011, 2015, 2018), whereas the $\delta^{18}O$ record from LSF 17 and LFS19 are new (Figures S3 and S4). All stalagmites in this study are composed of pure calcite (Figure S8) based on x-ray diffraction (XRD) analysis (Method S1).

### 2.3. U-Th dating

A total of 22 new subsamples (Table S1) of around 0.1 g were collected using a hand-drill in order to construct a linear age-model for the LSF17 and LSF19 stalagmites. The dates were obtained using a multicollector inductively coupled plasma mass spectrometer (MC-ICP-MS - Thermo-Finnigan NEPTUNE), at the University of Minnesota, following the procedure by Cheng et al. (2013b).

### 2.4. $\delta^{13}C$ and $\delta^{18}O$ analyses

Circa of 3000 analyses for $\delta^{18}O$ and $\delta^{13}C$ (Figure S3 and S4) were made using an isotope ratio mass spectrometer (IRMS) coupled to a gas bench system II, at the Stable Isotopes Laboratory of the Institute of Geosciences, University of São Paulo, Brazil. Aliquots of subsamples were collected using a micromill driller along the central axis of the stalagmites. Isotope ratios are expressed in $\delta$-notation, with per mil deviation from the Vienna Pee Dee Belemnite (VPDB) standard for carbonates.

### 2.5. $^{87}Sr/^{86}Sr$ analyses

A total of 48 subsamples from the LSF record were collected using a micromill Sherline 5400 model. Additionally, three samples from the carbonate host rock and four samples from different depths of the soil cover above the cave were also collected (Figure S7). All the analyses were made using a thermal ionization mass spectrometer (TIMS Finnigan MAT-262), at the Geochronology Laboratory of the University of Brasilia, Brazil. Precision was better than 0.001% ($2\sigma$) using a NIST SRM-987 standard. For the LSF record, around 20 mg per subsample was dissolved in 5% $HNO_3$ and 1 μL of the resulting solution was put into the rhenium filaments, where the sample is evaporated. Initially, the current was set to 0.3 A and then increased to 1.3 A in order to completely evaporate the solution. For the host rock and soil cover, around 50 mg per sample was crushed, weighted and stored in Teflon crucibles before analyzing it.

## 3. Results

### 3.1. U-Th dating

The LSF17 record has top and bottom ages of 4.86 ka and 7.47 ka BP and the LSF19 record has 1.05 ka and 11.17 ka BP, respectively, with most dating errors ($2\sigma$) < 1% (Table S1). Together with dates previously published by Stríkis et al. (2015), the full LSF record now extends between 27 ka and 1 ka BP (Fig. 2), with overlapping periods between them (Figure S3). The LSF record's average growth rate is 0.1323 mm/yr, with minimum of 0.001 mm/yr and maximum of 0.77341 mm/yr.

### 3.2. $\delta^{13}C$ and $\delta^{18}O$ analyses

The LSF record covers the period between 27 ka and 1 ka BP, with exception of hiatus between 8 ka and 7.6 ka BP, 23.7 ka and

**Fig. 1.** Shaded terrestrial ecoregions (Olson et al., 2001). Blue star - LSF and LG caves (this study; Stríkis et al., 2018), blue circle - JAR cave (Novello et al., 2019), red circle - RN caves (Utida et al., 2020), purple square - São José Palm swamp and Lagoa Feia (Cassino et al., 2018, 2020), navy blue square - Laguna La Gaiba (Whitney et al., 2011; Fornace et al., 2016).

22.8 ka BP, and a stalagmite gap between 12.1 ka and 11.2 ka BP (Fig. 2). The average temporal resolution is 13.2 yrs, with maximum of 3.1 yrs and minimum of 36.6 yrs. The $\delta^{13}C$ values are more positive between 27 ka and 17.3 ka BP, averaging circa 1.3‰, and reaching a maximum of 4.9‰ at 22.8 ka BP and, occasionally, outlier values reach more negative levels as −2.2‰ at 25.2 ka BP. The period between 18.1 ka and 16.4 ka BP is characterized by a shift from −0.9‰ up to 4.6‰, followed by a second shift from 2.8‰ down to −7.1‰ between 15.6 ka and 14.5 ka BP. The $\delta^{13}C$ during the late deglaciation and early Holocene, however, show less variability and more negative values, especially after 15 ka BP, when values drop to circa −6‰ and average negative values of −4.3‰, followed by slightly more negative values of circa −4‰ during the late-mid Holocene. The LG $\delta^{13}C$ record covers the Holocene, including a continuous growth during the hiatus found in the LSF19 record between 8 ka and 7.6 ka BP. It reproduces the same trend found in the LSF record, with slightly more positive values during the early Holocene, followed by more negative values during late-mid Holocene (Figure S4). Minor differences in the timing of identical shifts between samples LSF15 and LSF16 during the deglaciation are probably related to fewer dated samples at the base of the LSF15 sample, resulting in different growth rates inferred by linear age models near circa 15 ka BP.

In summary, the LSF $\delta^{18}O$ and $\delta^{13}C$ records can be subdivided into: the LGM phase between 27 ka and 19 ka BP, with average values of −5.55‰ and 1.27‰, respectively; the Deglacial phase between 19 ka and 11.7 ka BP with average values of −6.28‰ and −1.64‰, respectively; and the Holocene phase between 11.7 ka and 1 ka BP, with average values of −5.33‰ and −4.89‰, respectively. In addition, the LSF and LG $\delta^{13}C$ records show a synchronous transition to more negative values from early to mid-late Holocene around 6 ka BP, from −4.3 to −5.4‰ and from −7.5 to −9.7‰, respectively (Figure S4). Overall, the LSF record presents a transition from large-amplitude swings alternating between positive and negative values during the LGM, to more stable conditions after 15 ka BP. The record also shows that differences between $\delta^{13}C$ and $\delta^{18}O$ were as high as 10.2‰ during the LGM and, with the exception of a few short periods between 15.6 ka and 12 ka BP, this difference became less than 2‰ since the deglaciation.
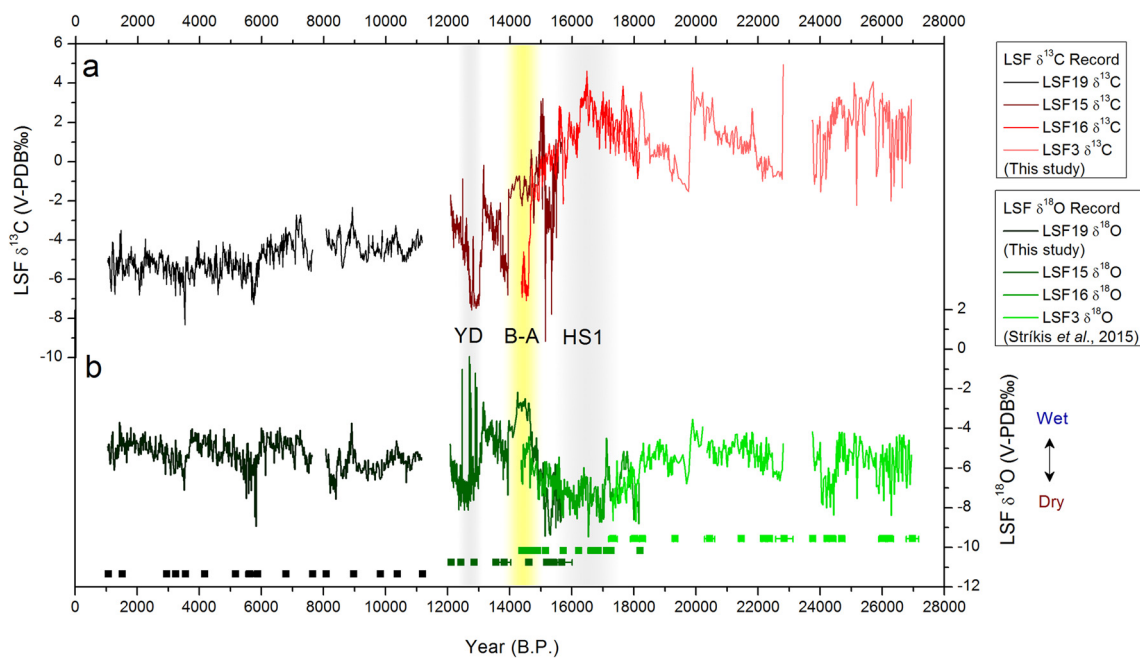
**Fig. 2.** (a) $\delta^{13}$C and (b) $\delta^{18}$O records from the LSF cave with its respective ages. YD - Younger Dryas, B-A - Bølling-Allerød, HS1 - Heinrich Stadial 1 are highlighted by gray and yellow shading, respectively.

## 3.3. $^{87}$Sr/$^{86}$Sr analyses

The $^{87}$Sr/$^{86}$Sr LSF record shows minor variations during the LGM until the early deglaciation, with an average value of 0.70842 (average error $\pm$ 0.00002), but rising during the late deglaciation to 0.71031 (average error $\pm$ 0.00007) and during the Holocene (Fig. 3) (Table S2). Analyses of the two end-members (Figure S7) show that the soil cover above the cave has an average value of 0.79184 (average error $\pm$ 0.00002), with higher radiogenic values in the deepest portion of the soil profile; whereas the host rock has a lower average value of 0.70826 (average error $\pm$ 0.0001) (Table S3), which is within the range of values from previous studies for the Lagoa do Jacaré Formation, reported to extend between 0.70740-0.70820 (Misi et al., 2007).

## 4. Proxy interpretations

Based on the environmental monitoring of caves, isotopic composition of local rainfall, cave drip water, and its correlation with regional rainfall and model experiments, the $\delta^{18}$O from stalagmites within the Central Brazil region is interpreted as a proxy of monsoon activity, with low $\delta^{18}$O values related to a strong monsoon and vice-versa (Vuille et al., 2012; Novello et al., 2016, 2017, 2018; Stríkis et al., 2011, 2015, 2018; Azevedo et al., 2019). Furthermore, previous $\delta^{18}$O studies in stalagmites from the LSF and LG caves showed a coupling between the strong phases of SAMS activity with cold events recorded in the Northern Hemisphere, such as the Heinrich Stadials during the glacial periods (Stríkis et al., 2015, 2018), and Bond events during the Holocene period (Stríkis et al., 2011), which are likely induced by an intensification of the North Atlantic Subtropical High, increasing the advection of moisture into the South American continent.

$\delta^{13}$C in speleothems, on the other hand, has been interpreted as a proxy for the contribution of the host-rock to the drip water, degree of prior calcite precipitation (PCP), changes between photosynthetic plant type and soil organic matter content, and in-cave kinetic fractionation, which are driven by change in temperature and air ventilation (Baker et al., 1997; McDermott, 2004; Mickler et al., 2006; Dreybrodt and Scholz, 2011; Azevedo et al., 2019;

Fohlmeister et al., 2020; Novello et al., 2021). Variations in the atmospheric pCO$_2$, however, can also exert a strong role in the photosynthetic discrimination and, consequently, the $\delta^{13}$C values of the vegetation-soil imprint in the epikarst, thereby potentially altering the $\delta^{13}$C signal from speleothems (Schubert and Jahren, 2012; Meyer et al., 2014; Wong and Breecker, 2015; Breecker, 2017; Novello et al., 2019). Furthermore, dripping rates can also play an important role over the $\delta^{13}$C from speleothems. During dry (wetter) periods, a reduction (increasing) in dripping rate results in an increase (decrease) in time for the solution to re-equilibrate with the cave atmosphere, which can increase (decrease) the $\delta^{13}$C of the precipitate (Dreybrodt and Scholz, 2011). Even though $\delta^{13}$C values in stalagmites can be affected by many factors, the combination of these forcings can provide a positive feedback, fractionating the $\delta^{13}$C values in the same direction: low soil organic matter content, sparse vegetation and predominance of grasslands with photosynthetic pathway C4 above the cave during dry conditions and increasing PCP contribute to enrichment of $\delta^{13}$C values in stalagmites; while high soil organic matter content, dense vegetation and predominance of trees with photosynthetic C3 pathway above the cave during wet conditions and decreasing PCP favor depletion of $\delta^{13}$C values (Novello et al., 2019 and references therein).

$^{87}$Sr/$^{86}$Sr in speleothems from South America have been used as proxies for water-rock interaction and the contribution from different end members, such as soil and host-rock (Wortham et al., 2017; Ward et al., 2019; Novello et al., 2019; Utida et al., 2020). The thinner soil during the LGM phase results in lower $^{87}$Sr/$^{86}$Sr values in the LSF record, with higher contribution from the bedrock into the speleothems. In this scenario, the epikarst environment is characterized by low organic matter content and sparser vegetation, which matches with the higher $\delta^{13}$C values found during the same period. On the other hand, the thicker soil and denser vegetation during the Holocene phase provide generally higher $^{87}$Sr/$^{86}$Sr values derived by higher soil organic matter content and lower $\delta^{13}$C values into the stalagmite record.

Additional forcings can potentially influence the $^{87}$Sr/$^{86}$Sr and $\delta^{13}$C in stalagmites; nonetheless, the overall values and coherence between proxies in the case of the LSF record, matches with the scenario described above. This same scenario was documented in
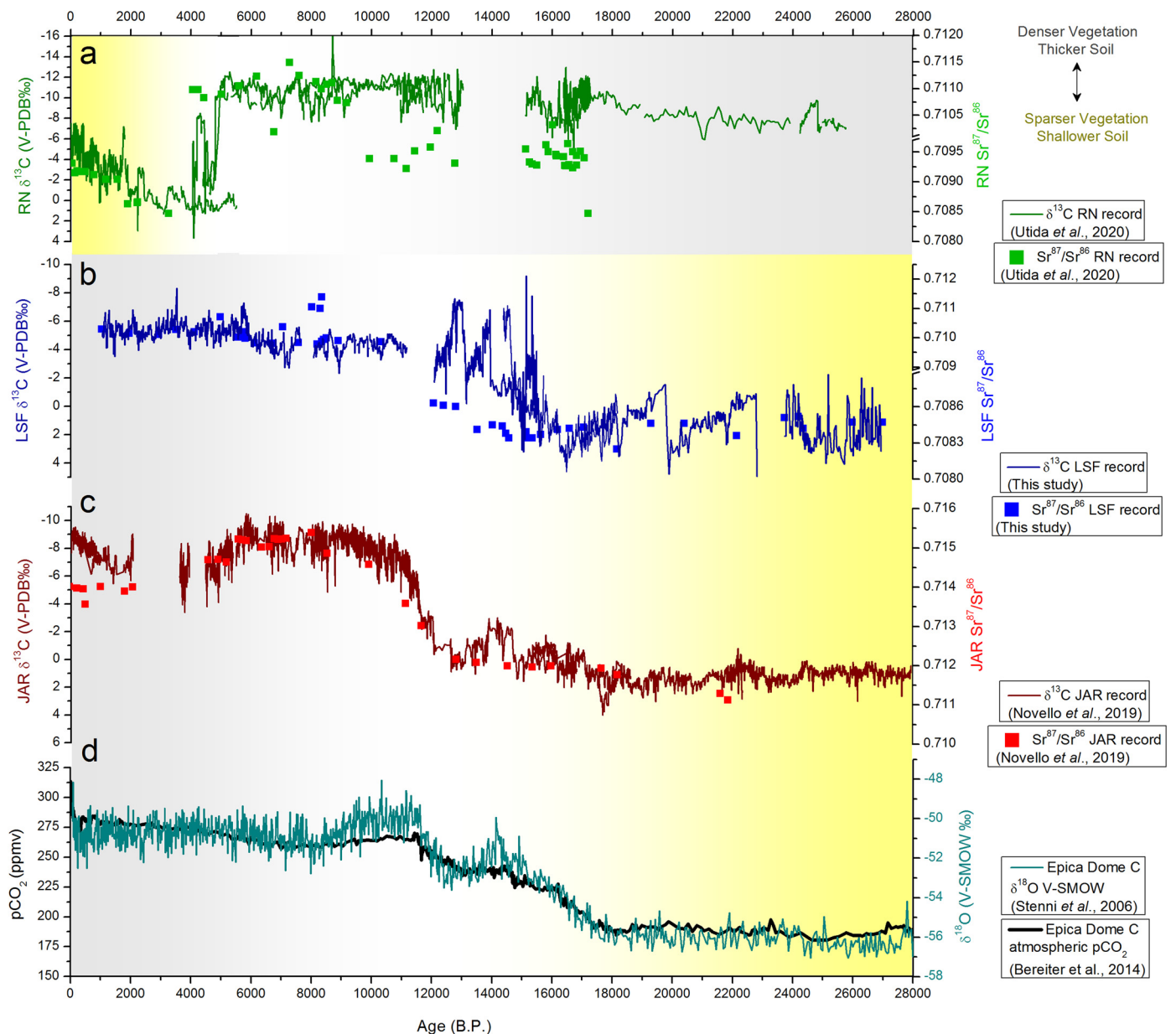
**Fig. 3.** Comparison of $\delta^{13}$C and $^{87}$Sr/$^{86}$Sr records from the (a) RN (Utida et al., 2020), (b) LSF (this study) and (c) JAR (Novello et al., 2019) caves and the influence of atmospheric pCO$_2$ (Bereiter et al., 2015) and global temperature based on $\delta^{18}$O (Stenni et al., 2006) from (d) Epica Dome C. Different transitions from sparse vegetation and shallower soil (light yellow) to denser vegetation and thicker soil (light gray) are indicated between the regions.

the JAR record, in central-western Brazil (Novello et al., 2019), and the same relationship between $^{87}$Sr/$^{86}$Sr, $\delta^{13}$C, soil and vegetation dynamics was also found in the RN record (Utida et al., 2020), in northeastern Brazil.

## 5. Discussion

The $\delta^{18}$O LSF record is sensitive to the millennial-scale events Heinrich Stadial 1, Bølling-Allerød and Younger Dryas, which are recorded during the LGM-Holocene transition (Stríkis et al., 2015, 2018). The record, however, presents similar average values during the LGM and the Holocene ($-5.5$‰ and $-5.3$‰ respectively), indicating similar SAMS intensities (Fig. 2). Similar conditions are also found during the Holocene in the $\delta^{18}$O from the LG record (Figure S4a). On the other hand, the $\delta^{13}$C LSF record shows an overall change, at circa 15 ka BP, from more positive values during the LGM to more negative values during the Holocene. This change is also recorded in the $^{87}$Sr/$^{86}$Sr, where lower radiogenic values are

found during the LGM when compared to the Holocene (Fig. 3). The decoupling of $\delta^{18}$O from the $\delta^{13}$C and $^{87}$Sr/$^{86}$Sr records suggests that monsoon activity was not the primarily driver of soil and vegetation change at the LSF site, at least on a Glacial-Interglacial scale; thus, other forcings, not exclusively related to paleoprecipitation and the monsoon activity forced this LGM-Holocene transition.

The $\delta^{13}$C and $^{87}$Sr/$^{86}$Sr shift found in the LSF record is similar to the one found in the JAR record, located in central-western Brazil (Novello et al., 2019). During the LGM, both the LSF and JAR records have more positive average $\delta^{13}$C and lower $^{87}$Sr/$^{86}$Sr values, followed by more negative average $\delta^{13}$C and higher $^{87}$Sr/$^{86}$Sr values during the Holocene (Fig. 3). Thus, suggesting that both regions are characterized by a transition from sparser vegetation, thinner soil, less radiogenic contribution above the cave during the LGM to denser vegetation, thicker soil, and higher radiogenic contribution during the late Deglacial-Holocene phases. These similarities indicate that common forcings acted in central-eastern and
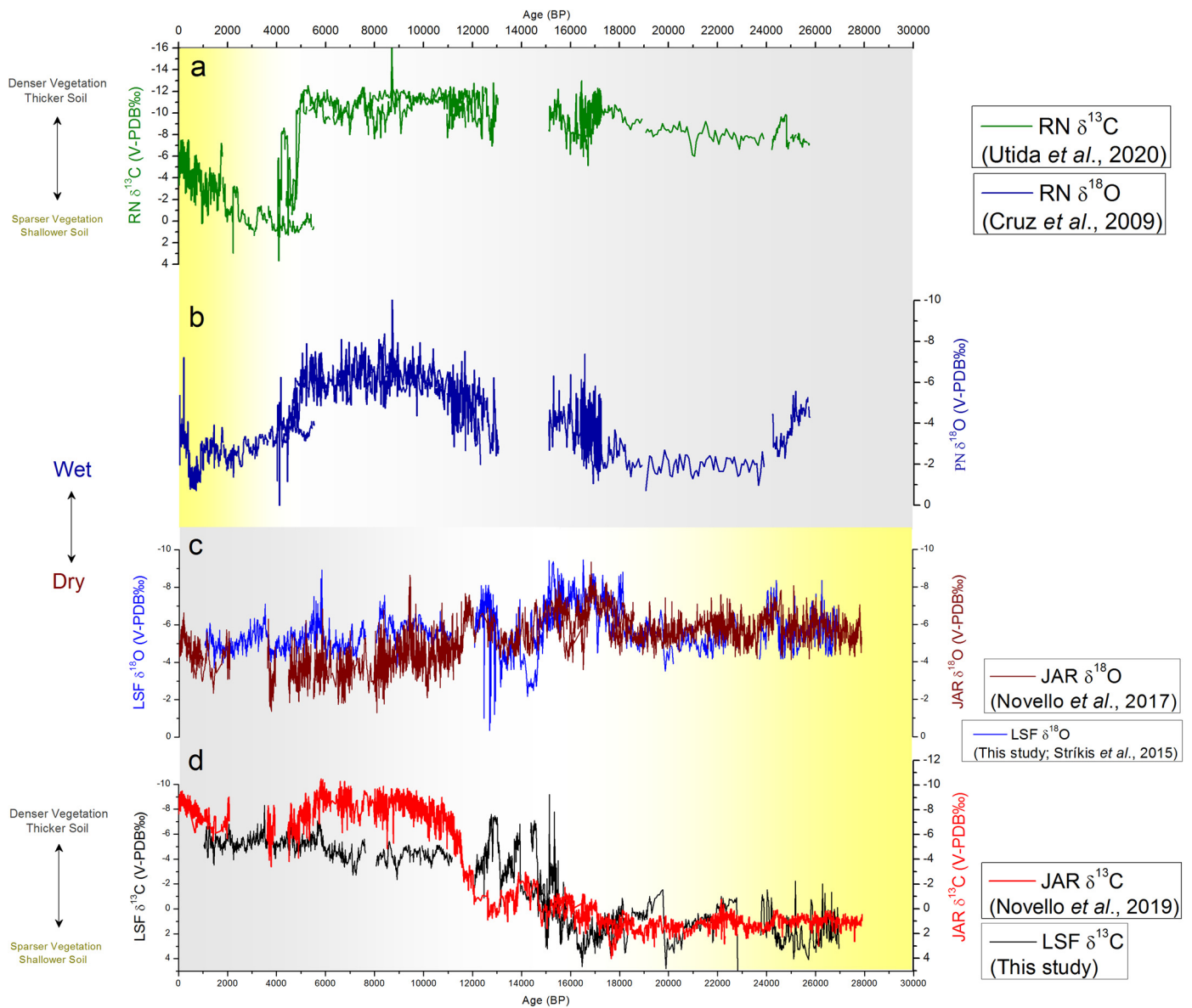
**Fig. 4.** Comparison between the $\delta^{13}C$ and $\delta^{18}O$ records from the (a, b) RN cave (Cruz et al., 2009; Utida et al., 2020), (c, d) the LSF cave (this study; Stríkis et al., 2015), and (c, d) the JAR cave (Novello et al., 2017, 2019), indicating a bipolar paleovegetation pattern of denser vegetation and thicker soil (light gray) contrasting with sparser vegetation and shallower soil (light yellow) during the LGM-Holocene transition.

central-western Brazil. The $\delta^{18}O$ records, however, are not similar. The JAR record shows more negative average $\delta^{18}O$ values during the LGM phase in comparison to the Holocene, suggesting stronger monsoon activity in the former than the latter, whereas the average $\delta^{18}O$ values from the LSF record show smaller differences in average values between the two phases (Fig. 4). Thus, reinforcing our hypothesis that change in precipitation solely could not explain the LGM-Holocene transition found in the Cerrado region of central-eastern (LSF) and central-western (JAR) Brazil. The similar $\delta^{18}O$ average values found in the LSF record between the LGM and Holocene are expected, due to its location in the center of the precipitation dipole axis previously described in South America during the LGM-Holocene transition (Cruz et al., 2009; Cheng et al., 2013a). Thus, this paleoclimate dipole did not seem to influence the paleovegetation during the LGM-Holocene transition. Furthermore, the multiproxy study by Novello et al. (2019) in the JAR cave already pointed out the decoupling between the SAMS variability and the epikarst vegetation-soil development during the LGM-Holocene transition. The authors associated the flourishing

of vegetation during the Holocene phase with the global increase of atmospheric $pCO_2$ during the deglaciation, with possible feedbacks from temperature and changes in local precipitation amount and/or seasonality (Fig. 4). A similar timing during the transition between the LGM and Holocene of the LSF $\delta^{13}C$ record and Epica Dome C atmospheric $pCO_2$ (Bereiter et al., 2015) normalized curves reinforce the notion that $pCO_2$ was the major modulator for our site (Figure S5). During the Holocene, however, when the atmospheric $pCO_2$ values were stabilized, the proxies from LSF record seem to coincide, suggesting a closer relationship between the monsoon intensity, local hydrology and vegetation/soil dynamics.

Conversely, this common trend found in the $\delta^{13}C$ and $^{87}Sr/^{86}Sr$ records from the LSF and JAR caves is opposite to the one found in stalagmite records from a cave system located in the Northeast Brazil region (Utida et al., 2020). The composite of $\delta^{13}C$ and $^{87}Sr/^{86}Sr$ records from these stalagmites (RN record hereafter), along with evidence from cave sediments and other near-lacustrine and marine records, indicate denser vegetation and thicker soil between the late LGM and the mid-Holocene, transitioning to sparser
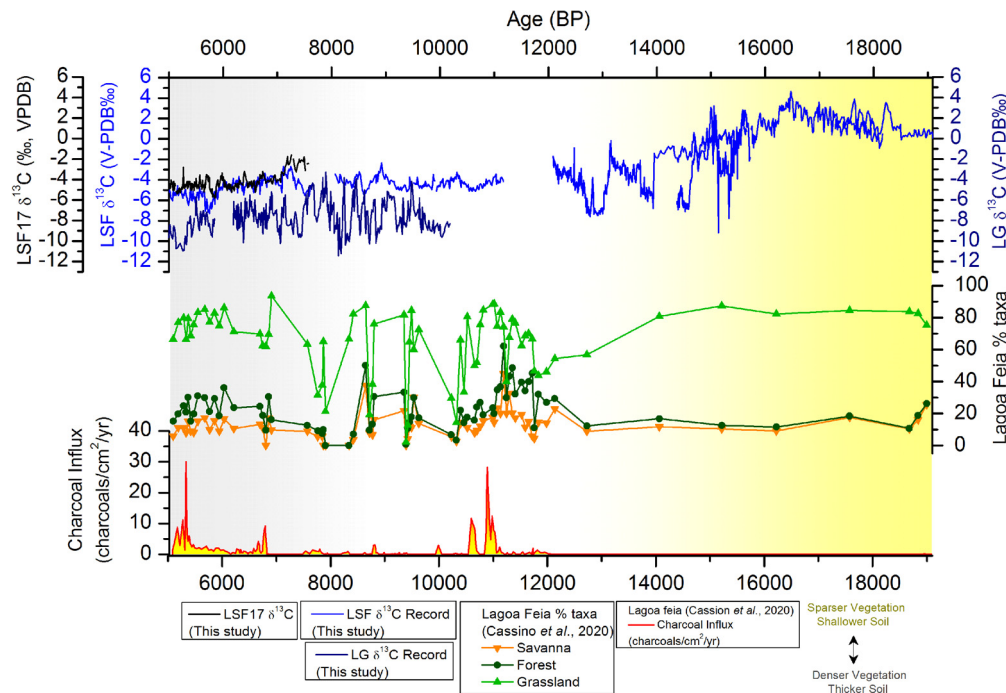
**Fig. 5.** Comparison between the LSF and LG records (this study) with Lagoa Feia pollen and charcoal records (Cassino et al., 2020) showing similar timing of the LGM-Holocene transition and expansion of vegetation roughly between 15-13 ka (B.P.) in Lagoa Feia and circa 15 ka (B.P.) in the LSF cave, when $\delta^{13}$C drops to Holocene average negative values.

vegetation and thinner soil after circa 4.2 ka (B.P.). This transition occurs simultaneously with an increase in drier conditions, based on the increase of positive $\delta^{18}$O values from the RN records (Cruz et al., 2009; Utida et al., 2020) (Fig. 4).

The different relationship between the $\delta^{18}$O records and the $\delta^{13}$C and $^{87}$Sr/$^{86}$Sr records found between central-eastern and central-western regions in comparison to northeastern Brazil can be related to how these vegetation types respond to changes of their climate regimes. The Central region, where Cerrado is the predominant vegetation, has a semi-humid climate with relatively high average annual precipitation derived from the SACZ, especially during the mature monsoon phase between November and February (NDJF); whereas in the Northeast region, where Caatinga is the predominant vegetation, has a semi-arid climate with relatively low average annual precipitation originating primarily from the ITCZ, especially during the mature phase between March-May (MAM). Additionally, the $\delta^{13}$C values from the LSF and JAR records follow the increase in global atmospheric pCO$_2$ and temperature (Fig. 3), indicating that the Cerrado soil-vegetation transition through the Deglaciation might have been strongly influenced by the increase in global atmospheric pCO$_2$, with possible feedbacks from temperature and changes in precipitation seasonality; while the Caatinga vegetation was more sensitive to precipitation variability. Additionally, recent lacustrine studies conducted near the LSF cave site show a transition from cooler to warmer conditions and the development of current Cerrado *sensu stricto* vegetation roughly around 15-13 ka BP (Cassino et al., 2018, 2020), which is coherent with the beginning of the $\delta^{13}$C transition at circa 15 ka BP found in the LSF record (Fig. 5). This indicates an earlier change in the paleovegetation transition in central-eastern in comparison to central-western at circa 11.7 ka BP (Novello et al., 2019), and in northeast Brazil at circa 4.2 ka BP (Utida et al., 2020). During this period, a negative excursion in the LSF15 $\delta^{13}$C record is in agreement with wet events (lowering in the $\delta^{18}$O), associated to millennial-scale oscillations, peaking at 13.9 ka BP (during the time of Glacial Interstadial-1d) and during the Younger Dryas, from near 13.1 ka to 12.1 ka BP (Rasmussen et al., 2014) (Figure S3). In this

context, we highlight a wet excursion during the mid-Holocene, starting near 6 ka BP as observed in the LSF19 $\delta^{18}$O record. The wet event is followed by a marked transition in the $\delta^{13}$C towards negative values in the speleothems from LG and LSF caves. This timing is in agreement with pollen records from Cerrado vegetation located in the same region, which shows a trend towards wet conditions (Cassino et al., 2020). In this regard, we do not rule out the role of precipitation on drive changes in vegetation on millennial-scale oscillations.

Our study suggests the existence of a past regional pattern of Cerrado vegetation and soil development between 15 and 11.7 ka BP, evidenced by the $\delta^{13}$C and $^{87}$Sr/$^{86}$Sr of stalagmites and supported by other proxies from lacustrine records near the studied sites. This paleovegetation pattern is opposite to the one found in the Caatinga, based on records in the Northeast Brazil region (Utida et al., 2020), suggesting the existence of a vegetation seesaw between those two regions. These patterns are the product of different responses from the biomes to their respective climate regimes, resulting in different timings of the vegetation and soil development transition between the Cerrado and Caatinga biomes, with the former taking place independently from the climate dipole and SAMS activity.

## 6. Conclusions

The new paleoenvironmental reconstruction using multiproxy data from Lapa Sem Fim and Lapa Grande caves, located in the Cerrado portion of the central-eastern Brazil, points to a sparser vegetation and thinner soil cover during the Deglacial-LGM phases, transitioning to denser vegetation and thicker soil above the cave during the Holocene. These results are consistent with similar studies performed in central-western Brazil, also within the Cerrado biome. The strategic location of our study site near the Cerrado-Caatinga border, along with evidence from lacustrine records, allows us to define a vegetation seesaw between the central and northeastern regions of the South American Monsoon System, which, in the case of the former, varied independently

from the climate dipole between the regions during the LGM-Holocene transition.

Our multiproxy study reinforces the notion that the increasing atmospheric $pCO_2$ during this time, together with possible feedbacks from temperature and local precipitation/seasonality, played a major role in the change of vegetation and soil above Lapa Sem Fim cave and, possibly, in other regions of Cerrado. The denser vegetation was responsible for soil stabilization and development above the cave, which led to an increase in the stalagmites $^{87}Sr/^{86}Sr$ values due to higher radiogenic contribution from the epikarst into the cave from the LGM to the Holocene. The period of transition recorded in the stalagmites, beginning at circa 15 ka (B.P.) in central-eastern and circa 11.7 ka (B.P.) in central-western Brazil, is concomitant with the transition found in near lacustrine studies in central-eastern region, between 15 ka and 13 ka (B.P.). Thus, our results strengthen the premise that multiproxy stalagmite studies can be used as precise recorders of regional paleovegetation and paleoenvironmental change.

## CRediT authorship contribution statement

**Vitor Azevedo:** Conceptualization, Formal analysis, Investigation, Methodology, Visualization, Writing – original draft, Writing – review & editing. **Nicolás M. Strikis:** Conceptualization, Formal analysis, Investigation, Methodology, Project administration, Supervision, Visualization, Writing – review & editing. **Valdir F. Novello:** Conceptualization, Formal analysis, Supervision, Writing – review & editing. **Camila L. Roland:** Formal analysis, Investigation, Methodology. **Francisco W. Cruz:** Funding acquisition, Project administration, Resources, Writing – review & editing. **Roberto V. Santos:** Funding acquisition, Methodology, Resources, Validation. **Mathias Vuille:** Writing – review & editing. **Giselle Utida:** Writing – review & editing. **Fábio Ramos Dias De Andrade:** Formal analysis, Methodology, Validation. **Hai Cheng:** Funding acquisition, Methodology, Resources, Validation. **R. Lawrence Edwards:** Funding acquisition, Methodology, Resources, Validation, Writing – review & editing.

## Declaration of competing interest

The authors declare that they have no known competing financial interests or personal relationships that could have appeared to influence the work reported in this paper.

## Data availability

The dataset generated as part of this study will be archived in the PANGAEA Database.

## Acknowledgements

## Appendix A. Supplementary material

Supplementary material related to this article can be found online at https://doi.org/10.1016/j.epsl.2021.116880.

## References

Agência Nacional de Águas (ANA) - National Water Agency database, source: www.snirh.gov.br/hidroweb/.

Azevedo, V., Stríkis, N.M., Santos, R.A., de Souza, J.G., Ampuero, A., Cruz, F.W., de Oliveira, P., Iriarte, J., Stumpf, C.F., Vuille, M., Mendes, V.R., 2019. Medieval Climate Variability in the eastern Amazon-Cerrado regions and its archeological implications. Sci. Rep. 9 (1), 1–10.

Baker, A., Ito, E., Smart, P.L., McEwan, R.F., 1997. Elevated and variable values of 13C in speleothems in a British cave system. Chem. Geol. 136 (3–4), 263–270.

Bereiter, B., Eggleston, S., Schmitt, J., Nehrbass-Ahles, C., Stocker, T.F., Fischer, H., Kipfstuhl, S., Chappellaz, J., 2015. Revision of the EPICA Dome C CO2 record from 800 to 600 kyr before present. Geophys. Res. Lett. 42 (2), 542–549.

Breecker, D.O., 2017. Atmospheric pCO2 control on speleothem stable carbon isotope compositions. Earth Planet. Sci. Lett. 458, 58–68.

Cassino, R.F., Martinho, C.T., da Silva Caminha, S.A., 2018. A Late Quaternary palynological record of a palm swamp in the Cerrado of central Brazil interpreted using modern analog data. Palaeogeogr. Palaeoclimatol. Palaeoecol. 490, 1–16.

Cassino, R.F., Ledru, M.P., de Almeida Santos, R., Favier, C., 2020. Vegetation and fire variability in the central Cerrados (Brazil) during the Pleistocene-Holocene transition was influenced by oscillations in the SASM boundary belt. Quat. Sci. Rev. 232, 106209.

Cheng, H., Edwards, R.L., Hoff, J., Gallup, C.D., Richards, D.A., Asmerom, Y., 2000. The half-lives of uranium-234 and thorium-230. Chem. Geol. 169 (1–2), 17–33.

Cheng, H., Sinha, A., Cruz, F.W., Wang, X., Edwards, R.L., d'Horta, F.M., Ribas, C.C., Vuille, M., Stott, L.D., Auler, A.S., 2013a. Climate change patterns in Amazonia and biodiversity. Nat. Commun. 4 (1), 1–6.

Cheng, H., Edwards, R.L., Shen, C.C., Polyak, V.J., Asmerom, Y., Woodhead, J., Hellstrom, J., Wang, Y., Kong, X., Spötl, C., Wang, X., 2013b. Improvements in $^{230}Th$ dating, $^{230}Th$ and $^{234}U$ half-life values, and U–Th isotopic measurements by multi-collector inductively coupled plasma mass spectrometry. Earth Planet. Sci. Lett. 371, 82–91.

Cruz, F.W., Burns, S.J., Karmann, I., Sharp, W.D., Vuille, M., Cardoso, A.O., Ferrari, J.A., Dias, P.L.S., Viana, O., 2005. Insolation-driven changes in atmospheric circulation over the past 116,000 years in subtropical Brazil. Nature 434 (7029), 63–66.

Cruz, F.W., Vuille, M., Burns, S.J., Wang, X., Cheng, H., Werner, M., Edwards, R.L., Karmann, I., Auler, A.S., Nguyen, H., 2009. Orbitally driven east–west antiphasing of South American precipitation. Nat. Geosci. 2 (3), 210–214.

Dreybrodt, W., Scholz, D., 2011. Climatic dependence of stable carbon and oxygen isotope signals recorded in speleothems: from soil water to speleothem calcite. Geochim. Cosmochim. Acta 75 (3), 734–752.

Fohlmeister, J., Voarintsoa, N.R.G., Lechleitner, F.A., Boyd, M., Brandtstätter, S., Jacobson, M.J., Oster, J., 2020. Main controls on the stable carbon isotope composition of speleothems. Geochim. Cosmochim. Acta 279, 67–87.

Fornace, K.L., Whitney, B.S., Galy, V., Hughen, K.A., Mayle, F.E., 2016. Late Quaternary environmental change in the interior South American tropics: new insight from leaf wax stable isotopes. Earth Planet. Sci. Lett. 438, 75–85.

McDermott, F., 2004. Palaeo-climate reconstruction from stable isotope variations in speleothems: a review. Quat. Sci. Rev. 23 (7–8), 901–918.

Meyer, K.W., Feng, W., Breecker, D.O., Banner, J.L., Guilfoyle, A., 2014. Interpretation of speleothem calcite $\delta$13C variations: evidence from monitoring soil CO2, drip water, and modern speleothem calcite in central Texas. Geochim. Cosmochim. Acta 142, 281–298.

Mickler, P.J., Stern, L.A., Banner, J.L., 2006. Large kinetic isotope effects in modern speleothems. Geol. Soc. Am. Bull. 118 (1–2), 65–81.

Misi, A., Kaufman, A.J., Veizer, J., Powis, K., Azmy, K., Boggiani, P.C., Gaucher, C., Teixeira, J.B.G., Sanches, A.L., Iyer, S.S., 2007. Chemostratigraphic correlation of Neoproterozoic successions in South America. Chem. Geol. 237 (1–2), 143–167.

Novello, V.F., Vuille, M., Cruz, F.W., Stríkis, N.M., De Paula, M.S., Edwards, R.L., Cheng, H., Karmann, I., Jaqueto, P.F., Trindade, R.I., Hartmann, G.A., 2016. Centennial-scale solar forcing of the South American Monsoon System recorded in stalagmites. Sci. Rep. 6 (1), 1–8.

Novello, V.F., Cruz, F.W., Vuille, M., Stríkis, N.M., Edwards, R.L., Cheng, H., Emerick, S., De Paula, M.S., Li, X., Barreto, E.D.S., Karmann, I., 2017. A high-resolution history of the South American Monsoon from Last Glacial Maximum to the Holocene. Sci. Rep. 7 (1), 1–8.

Novello, V.F., Cruz, F.W., Moquet, J.S., Vuille, M., de Paula, M.S., Nunes, D., Edwards, R.L., Cheng, H., Karmann, I., Utida, G., Stríkis, N.M., 2018. Two millennia of South Atlantic Convergence Zone variability reconstructed from isotopic proxies. Geophys. Res. Lett. 45 (10), 5045–5051.

Novello, V.F., Cruz, F.W., McGlue, M.M., Wong, C.I., Ward, B.M., Vuille, M., Santos, R.A., Jaqueto, P., Pessenda, L.C., Atorre, T., Ribeiro, L.M., 2019. Vegetation and environmental changes in tropical South America from the last glacial to the Holocene documented by multiple cave sediment proxies. Earth Planet. Sci. Lett. 524, 115717.

Novello, V.F., Cruz, F.W., Vuille, M., Campos, J.L.P.S., Stríkis, N.M., Apaéstegui, J., Moquet, J.S., Azevedo, V., Ampuero, A., Utida, G., Wang, X., 2021. Investigating $\delta$13C values in stalagmites from tropical South America for the last two millennia. Quat. Sci. Rev. 255, 106822.

Olson, D.M., Dinerstein, E., Wikramanayake, E.D., Burgess, N.D., Powell, G.V., Underwood, E.C., D'amico, J.A., Itoua, I., Strand, H.E., Morrison, J.C., Loucks, C.J., 2001. Terrestrial Ecoregions of the World: A New Map of Life on Earth: a new global map of terrestrial ecoregions provides an innovative tool for conserving biodiversity. Bioscience 51 (11), 933–938.

Rasmussen, S.O., Bigler, M., Blockley, S.P., Blunier, T., Buchardt, S.L., Clausen, H.B., Cvijanovic, I., Dahl-Jensen, D., Johnsen, S.J., Fischer, H., Gkinis, V., 2014. A stratigraphic framework for abrupt climatic changes during the Last Glacial period based on three synchronized Greenland ice-core records: refining and extending the INTIMATE event stratigraphy. Quat. Sci. Rev. 106, 14–28.

Santos, R.V., De Alvarenga, C.J.S., Dardenne, M.A., Sial, A.N., Ferreira, V.P., 2000. Carbon and oxygen isotope profiles across Meso-Neoproterozoic limestones from central Brazil: Bambuí and Paranoá groups. Precambrian Res. 104 (3–4), 107–122.

Schubert, B.A., Jahren, A.H., 2012. The effect of atmospheric CO2 concentration on carbon isotope fractionation in C3 land plants. Geochim. Cosmochim. Acta 96, 29–43.

Shen, C.C., Wu, C.C., Cheng, H., Edwards, R.L., Hsieh, Y.T., Gallet, S., Chang, C.C., Li, T.Y., Lam, D.D., Kano, A., Hori, M., 2012. High-precision and high-resolution carbonate 230Th dating by MC-ICP-MS with SEM protocols. Geochim. Cosmochim. Acta 99, 71–86.

Stenni, B., Sachs, J.P., Selmo, E., Souchez, R., Steffensen, J.P., Udisti, R., Jouzel, J., Masson-Delmotte, V., Rothlisberger, R., Castellano, E., Cattani, O., 2006. EPICA dome C stable isotope data to 44.8 KYrBP. IGBP PAGES/World. Data Center for Paleoclimatology Data Contribution Series, 112.

Stríkis, N.M., Cruz, F.W., Cheng, H., Karmann, I., Edwards, R.L., Vuille, M., Wang, X., de Paula, M.S., Novello, V.F., Auler, A.S., 2011. Abrupt variations in South American monsoon rainfall during the Holocene based on a speleothem record from central-eastern Brazil. Geology 39 (11), 1075–1078.

Stríkis, N.M., Chiessi, C.M., Cruz, F.W., Vuille, M., Cheng, H., de Souza Barreto, E.A., Mollenhauer, G., Kasten, S., Karmann, I., Edwards, R.L., Bernal, J.P., 2015. Timing and structure of Mega-SACZ events during Heinrich Stadial 1. Geophys. Res. Lett. 42 (13), 5477–5484A.

Stríkis, N.M., Cruz, F.W., Barreto, E.A., Naughton, F., Vuille, M., Cheng, H., Voelker, A.H., Zhang, H., Karmann, I., Edwards, R.L., Auler, A.S., 2018. South American monsoon response to iceberg discharge in the North Atlantic. Proc. Natl. Acad. Sci. 115 (15), 3788–3793.

Utida, G., Cruz, F.W., Santos, R.V., Sawakuchi, A.O., Wang, H., Pessenda, L.C.R., Novello, V.F., Vuille, M., Strauss, A., Borella, A.C., Stríkis, N.M., Guedes, C.C.F., Andrade, F.R.D., Zhang, H., Cheng, H., Edwards, R.L., 2020. Climate changes in Northeastern Brazil from Deglacial to Maghalayan periods and related environmental impacts. Quat. Sci. Rev. 250, 106655.

Vuille, M., Burns, S.J., Taylor, B.L., Cruz, F.W., Bird, B.W., Abbott, M.B., Kanner, L.C., Cheng, H., Novello, V.F., 2012. A review of the South American Monsoon history as recorded in stable isotopic proxies over the past two millennia. Clim. Past 8, 1309–1321.

Wang, X., Auler, A.S., Edwards, R.L., Cheng, H., Cristalli, P.S., Smart, P.L., Richards, D.A., Shen, C.C., 2004. Wet periods in northeastern Brazil over the past 210 kyr linked to distant climate anomalies. Nature 432 (7018), 740–743.

Wang, X., Auler, A.S., Edwards, R.L., Cheng, H., Ito, E., Wang, Y., Kong, X., Solheid, M., 2007. Millennial-scale precipitation changes in southern Brazil over the past 90,000 years. Geophys. Res. Lett. 34 (23).

Ward, B.M., Wong, C.I., McGee, D., Santos, R.V., Silva, L.C., Cruz, F.W., Wang, X., Edwards, R.L., Cheng, H., 2019. Reconstruction of Holocene coupling between the South American Monsoon System and local moisture variability from speleothem $\delta$18O and 87Sr/86Sr records. Quat. Sci. Rev. 210, 51–63.

Whitney, B.S., Mayle, F.E., Punyasena, S.W., Fitzpatrick, K.A., Burn, M.J., Guillen, R., Chavez, E., Mann, D., Pennington, R.T., Metcalfe, S.E., 2011. A 45 kyr palaeoclimate record from the lowland interior of tropical South America. Palaeogeogr. Palaeoclimatol. Palaeoecol. 307 (1–4), 177–192.

Wong, C.I., Breecker, D.O., 2015. Advancements in the use of speleothems as climate archives. Quat. Sci. Rev. 127, 1–18.

Wortham, B.E., Wong, C.I., Silva, L.C., McGee, D., Montañez, I.P., Rasbury, E.T., Cooper, K.M., Sharp, W.D., Glessner, J.J., Santos, R.V., 2017. Assessing response of local moisture conditions in central Brazil to variability in regional monsoon intensity using speleothem 87Sr/86Sr values. Earth Planet. Sci. Lett. 463, 310–322.